

# $\gamma^*N \rightarrow N^*(1520)$ form factors in the timelike regime

G. Ramalho<sup>1</sup> and M. T. Peña<sup>2</sup>

<sup>1</sup>*International Institute of Physics, Federal University of Rio Grande do Norte, Campus Universitário - Lagoa Nova, CP. 1613, Natal, Rio Grande do Norte 59078-970, Brazil and*

<sup>2</sup>*Centro de Física Teórica e de Partículas (CFTP), Instituto Superior Técnico (IST), Universidade de Lisboa, Avenida Rovisco Pais, 1049-001 Lisboa, Portugal*

(Dated: October 16, 2021)

The covariant spectator quark model, tested before in a variety of electromagnetic baryon excitations, is applied here to the  $\gamma^*N \rightarrow N^*(1520)$  reaction in the timelike regime. The transition form factors are first parametrized in the spacelike region in terms of a valence quark core model together with a parametrization of the meson cloud contribution. The form factor behavior in the timelike region is then predicted, as well as the  $N^*(1520) \rightarrow \gamma N$  decay width and the  $N^*(1520)$  Dalitz decay,  $N^*(1520) \rightarrow e^+e^-N$ . Our results may help in the interpretation of dielectron production from elementary  $pp$  collisions and from the new generation of HADES results using a pion beam. In the  $q^2 = 0-1$  GeV<sup>2</sup> range we conclude that the *QED approximation* (a  $q^2$  independent form factor model) underestimates the electromagnetic coupling of the  $N^*(1520)$  from 1 up to 2 orders of magnitude. We conclude also that the  $N^*(1520)$  and  $\Delta(1232)$  Dalitz decay widths are comparable.

## I. INTRODUCTION

Measurements of dielectron production in elementary  $pp$  collisions [1–7] expand to the timelike region ( $q^2 > 0$ , where  $q$  is the momentum transfer) the extraordinarily precise results obtained with the electron scattering CLAS  $N^*$  program at Jefferson Lab [1, 8, 9], describing the electromagnetic structure of baryonic transitions in spacelike or  $q^2 < 0$  region (program to be extended down to  $-12$  GeV<sup>2</sup>, as well as up to  $-0.05$  GeV<sup>2</sup>). Although different, both experiments, with strong and electromagnetic probes, complement each other [1].

In the last years,  $pp$  and quasi-free  $pn$  reactions were combined for the determination of different medium effects, difficult to disentangle [10–12]. The dominance of the  $\Delta(1232)$  Dalitz decay for dielectron emission above the  $\pi^0$  mass was confirmed by HADES, by the simultaneous measurement of one pion-production channels [3, 4]. However, an excess of production with respect to the baryon and meson cocktail simulations was observed, an effect pointing to the contribution of low-lying resonances, as the  $N^*(1520)$  [3, 13, 14]. The important role of this state in dilepton decay reactions, as the  $\gamma^*N \rightarrow e^+e^-N$ , in the timelike region was also discussed in Refs. [2, 15–17].

To focus on this contribution, very recently, the High Acceptance Di-Electron Spectrometer (HADES) at GSI was combined with a pion beam for perfect and unique cold matter studies [3–5]. The first pion beam results from HADES experiments [13, 14] also show in the dielectron emission channel a large peak in the number of events in a missing mass range of 0.9–1.04 GeV<sup>2</sup>, which is expected to be due to  $N^*(1520)$  decay. The new experiments with HADES and a pion beam are an ex-

traordinary opportunity to shed light on the behavior of the second and third resonance region, and the resonance form factors in the timelike region [3, 13, 14]. This motivates calculations, as the one reported here, for the extraction of different contributions to  $e^+e^-$  emission, as well as to revisit, in the electromagnetic couplings of baryons, the extensively applied vector meson dominance principle and its validity. To understand the structure of hadrons from first principles the nonperturbative character of QCD at low energies and chiral symmetry have to be combined [8]. In the two extreme regimes of QCD – the low-energy regime where the energies are (much) smaller than a typical strong interaction scale and the high-energy regime where the energies are much higher than that scale – well-established theoretical methods Chiral Perturbation Theory (ChPT) and perturbative QCD, respectively, apply [8]. However, in the intermediate-energy regime some degree of modeling is still required.

Promising tools are Dyson-Schwinger-Faddeev functional methods and lattice QCD. Although progress in these fronts continues, they are developed in Euclidean space and, so far, are limited to the region below the  $\rho$ -meson pole [18]. At this stage, we take here a more phenomenological approach, based on the covariant spectator quark model. This model is based on the covariant spectator theory (CST) [19]. In a relatively successful and unifying way, our approach pictures a large variety of baryons as a superposition of a core of three valence quarks and meson cloud components [6–8, 20–33]. After a series of applications of the model to the electromagnetic excitation of baryons in the spacelike regime, we analyzed also the impact of the  $\Delta(1232)$  resonance in the timelike reactions [6, 7].

In this work we start with the quark model described in Ref. [20] for the  $N^*(1520)$  resonance and extend it to the region  $q^2 > 0$ . In addition to the contribution from the bare core, we take also a meson cloud contribution. This contribution is modeled within the lines of our previous study of the  $\Delta(1232)$  in the timelike region, i.e., with the pion-photon coupling parametrized by the pion form factor data [7].

Three conclusions emerged in the context of our model: i) the  $\gamma^*N \rightarrow N^*(1520)$  timelike transition form factors are dominated by the meson cloud contributions; ii) in the range  $q^2 = 0-1 \text{ GeV}^2$  the constant form factor model (also known as *QED approximation*) usually taken in the literature underestimates the electromagnetic coupling of the  $N^*(1520)$  with consequences for the differential Dalitz decay width; iii) in addition to the  $\Delta(1232)$  resonance the  $N^*(1520)$  has a role in dilepton decay reactions at intermediate energies.

This article is organized as follows: In Sec. II we describe the methodology used to extend a valence quark model fixed in the spacelike region to the timelike region. Next, in Sec. III, we discuss the relation between the  $\gamma^*N \rightarrow N^*(1520)$  form factors and the formulas for the photon and Dalitz decay widths of the  $N^*(1520)$ . The formalism of the covariant spectator quark model used here is presented briefly in Sec. IV. In Sec. V we discuss the formulas used to calculate the  $\gamma^*N \rightarrow N^*(1520)$  form factors. The results for the form factors in the timelike region and the  $N^*(1520)$  decay widths are presented in Sec. VI. Outlook and conclusions are presented in Sec. VII.

## II. METHODOLOGY

In the covariant spectator quark model, the application of impulse approximation to the interaction of a photon with a baryon, seen as a three quark  $qqq$  state, justifies that one integrates out the relative internal momentum in the spectator diquark subsystem [21, 25, 26]. After this internal momentum integration, in the process of the covariant integration over the global momentum of the interacting diquark one may keep only the main contribution, which is originated by the on-mass-shell pole of the diquark — while the remaining quark that interacts with the photon is taken to be off-mass-shell [25]. This last integration on the on-shell diquark internal momenta amounts to having the  $qqq$  system as a quark-diquark system, and to treating the diquark with an effective average mass  $m_D$  [21, 25, 26]. It is also an ingredient of the model that the electromagnetic quark current is represented by a parametrization of vector meson dominance [21, 26, 34, 35]. In addition to the contributions from the core of valence quarks, the covariant spectator quark model can include also a covariant parametrization of the meson cloud effects that are important in the low momentum transfer region and that depend on the baryons participating in

the reaction [6, 7, 22, 23, 31, 36–38].

Here, the extension of the model to the timelike regime, requires two important modifications:

- The nucleon and the  $N^*(1520)$  quark core wave functions have to be calculated in timelike kinematic conditions, depending on an arbitrary mass  $W$  which can differ from the resonance mass, labeled  $M_R$ .
- The electromagnetic quark current has also to be extended to the timelike regime. That is done by introducing finite mass widths for the  $\rho$  and  $\omega$  mesons.

For the  $\gamma^*N \rightarrow \Delta(1232)$  transition in the timelike region we have already found that the meson cloud contributions are important, in comparison to the valence quark contributions [7]. It is worthwhile now to test whether the same phenomena occurs for the  $N^*(1520)$  resonance, which carries, in particular, a different isospin. In our model the valence quark contributions for the magnetic and electric form factors vanish at the photon point ( $q^2 = 0$ ) due to the orthogonality of the initial and final state wave functions [20]. Other valence quark model estimate them as non-zero contributions (a discussion can be found in Ref. [20]). Since in our model, the valence quark contributions for the electric and magnetic transition form factors vanish at  $q^2 = 0$ , their extension to the  $q^2 > 0$  region gives non-zero but small contributions for those transition form factors. Nevertheless, our model can provide a good approximation for the  $N^*(1520)$  resonance in the timelike region based on the meson cloud contributions, which dominate in the timelike region. Moreover, the form factors show a dependence on  $q^2$  with consequences for the analysis of reactions in the timelike region, where the electromagnetic couplings are often fixed at their value at  $q^2 = 0$  (*QED approximation*).

## III. $N^*(1520)$ DALITZ DECAY

The  $N^*(1520)$  resonance is a  $J^P = \frac{3}{2}^-$  state, with isospin  $I = \frac{1}{2}$ . The  $N^*(1520)$  Dalitz decay into the nucleon can be expressed in terms of the decay width [39]

$$\Gamma_{\gamma^*N}(q, W) = \frac{3\alpha}{16} \frac{(W - M)^2}{M^2 W^3} \sqrt{y_+ y_-} |G_T(q^2, W)|^2, \quad (3.1)$$

where  $q = \sqrt{q^2}$ ,  $\alpha$  is the fine-structure constant,

$$y_{\pm} = (W \pm M)^2 - q^2, \quad (3.2)$$

and  $|G_T(q^2, W)|^2$  is a combination of the electromagnetic transition form factors given by

$$|G_T(q^2, W)|^2 = 3|G_M(q^2, W)|^2 + |G_E(q^2, W)|^2 + \frac{q^2}{2W^2} |G_C(q^2, W)|^2. \quad (3.3)$$

In the previous equation  $G_M$ ,  $G_E$  and  $G_C$  are, respectively, the magnetic dipole, electric and Coulomb quadrupole form factors, which are complex functions in the region  $q^2 > 0$ .

The dilepton decay rate is obtained from the relation (3.1). Using the compact notation  $\Gamma \equiv \Gamma_{e^+e^-N}$ , one can calculate the dilepton decay rate [39, 40] as

$$\begin{aligned} \Gamma'_{e^+e^-N}(q, W) &\equiv \frac{d\Gamma}{dq}(q, W) \\ &= \frac{2\alpha}{3\pi q^3} (2\mu^2 + q^2) \sqrt{1 - \frac{4\mu^2}{q^2}} \Gamma_{\gamma^*N}(q, W), \end{aligned} \quad (3.4)$$

where  $\mu$  is the electron mass.

The Dalitz decay width is then determined by the integral of  $\Gamma'_{e^+e^-N}(q, W)$  in the kinematic region  $4\mu^2 \leq q^2 \leq (W - M)^2$ :

$$\Gamma_{e^+e^-N}(W) = \int_{2\mu}^{W-M} \Gamma'_{e^+e^-N}(q, W) dq. \quad (3.5)$$

#### IV. COVARIANT SPECTATOR QUARK MODEL

In the covariant spectator quark model the baryon wave functions are specified by the flavor, spin, orbital angular momentum and radial excitations of the quark-diquark states that are consistent with the baryon quantum number [8, 21, 26, 36]. The nucleon wave function  $\Psi_N$  was obtained in Ref. [21] and the wave function  $\Psi_R$  of the resonance  $N^*(1520)$  in Ref. [20]. Those wave functions describe only the valence quark content of those baryons.

The constituent quark electromagnetic current is written as the sum of a Dirac and a Pauli component,

$$\begin{aligned} j_q^\mu(q) &= \left( \frac{1}{6} f_{1+} + \frac{1}{2} f_{1-\tau_3} \right) \gamma^\mu + \\ &\quad \left( \frac{1}{6} f_{2+} + \frac{1}{2} f_{2-\tau_3} \right) \frac{i\sigma^{\mu\nu} q_\nu}{2M}, \end{aligned} \quad (4.1)$$

where  $\tau_3$  is the Pauli matrix that acts on the (initial and final) baryon isospin states,  $M$  is the nucleon mass, and  $f_{i\pm}(q^2)$  are the quark isoscalar/isovector form factors. Those form factors will be parametrized with a form consistent with the vector meson dominance (VMD) mechanism.

For inelastic reactions we replace  $\gamma^\mu \rightarrow \gamma^\mu - \frac{q q^\mu}{q^2}$ , in order to ensure the conservation of the transition current. This is equivalent to the Landau prescription [41–43]. The extra term restores current conservation but does not affect the results of the observables [41].

Once we know the wave functions for the nucleon  $\Psi_N(P_-, k)$  and the resonance  $\Psi_R(P_+, k)$ , with momenta  $P_-$  and  $P_+$ , respectively, and the diquark momentum  $k$ ,

we can calculate the transition current in a relativistic impulse approximation [21, 25, 26]

$$J^\mu = 3 \sum_{\Gamma} \int_k \bar{\Psi}_R(P_+, k) j_q^\mu \Psi_N(P_-, k), \quad (4.2)$$

where  $\Gamma$  represents the intermediate diquark polarizations, and the integration symbol represents the covariant integration over the diquark on-shell momentum. The factor 3 takes into account the contributions of all of the quark pairs. The polarization indices are suppressed in the wave functions just for simplicity. The current associated with the meson cloud will be parametrized separately and more phenomenologically, as discussed later. The two components of the current are conserved individually.

The definition (4.2) for the electromagnetic current is valid for the spacelike and timelike regions. In the rest frame of the resonance (mass  $W$ ), we may write

$$P_- = (E_N, -\mathbf{q}), \quad P_+ = (W, \mathbf{0}), \quad (4.3)$$

where  $\mathbf{q}$  is the photon three-momentum. In that case the magnitude of the three-vector  $\mathbf{q}$  corresponding to a photon of four-momentum  $q$ , and the squared momentum  $q^2$ , is given by

$$|\mathbf{q}|^2 = \frac{y_+ y_-}{4W^2}, \quad (4.4)$$

where  $y_{\pm}$  is defined in Eq. (3.2). In the case of a timelike photon ( $q^2 > 0$ ), the last condition implies that physical photons (with  $|\mathbf{q}|^2 \geq 0$ ) are defined only for  $0 \leq q^2 \leq (W - M)^2$ , or  $q^2 \geq (W + M)^2$ . As we are interested in resonance decay, the region near  $q^2 = 0$  is the one where we will focus, and we will skip the discussion of the last case. In conclusion, because both the nucleon and the resonance are taken on their mass-shell the transition form factors for a transition between a nucleon of mass  $M$  and a resonance of mass  $W$  are kinematically restricted to the region  $q^2 \leq (W - M)^2$  in the timelike region. As the resonance mass  $W$  grows larger, the spanned momentum region increases.

#### A. Quark form factors

The valence quark form factors, included in the effective electromagnetic quark current (4.1) have a parametrization inspired in the VMD mechanism that reads [21, 34, 35]

$$\begin{aligned} f_{1\pm}(q^2) &= \lambda_q + (1 - \lambda_q) \frac{m_{v\pm}^2}{m_{v\pm}^2 - q^2} - c_{\pm} \frac{M_h^2 q^2}{(M_h^2 - q^2)^2}, \\ f_{2\pm}(q^2) &= \kappa_{\pm} \left\{ d_{\pm} \frac{m_{v\pm}^2}{m_{v\pm}^2 - q^2} + (1 - d_{\pm}) \frac{M_h^2}{M_h^2 - q^2} \right\}. \end{aligned} \quad (4.5)$$

Here,  $m_{v\pm}$  represents light vector meson masses,  $M_h$  is an effective heavy vector meson,  $\kappa_{\pm}$  indicates the quark

anomalous magnetic moment,  $c_{\pm}, d_{\pm}$  are mixture coefficients, and  $\lambda_q$  is a high-energy parameter related to the quark density number in the deep inelastic limit [21]. For the isoscalar functions one has  $m_{v+} = m_{\omega}$  ( $\omega$  mass) and for the isovector functions one uses  $m_{v-} = m_{\rho}$  ( $\rho$  mass). The term in  $M_h = 2M$  simulates the effects of the heavier mesons and, therefore, all short range physics.

Specifically, we used the quark current parametrization of model II from Ref. [21]:  $\lambda_q = 1.21$ ,  $c_+ = 4.16$ ,  $c_- = 1.16$ ,  $d_+ = d_- = -0.686$ ,  $\kappa_+ = 1.639$  and  $\kappa_- = 1.833$ . The values were adjusted in order to describe the nucleon elastic form factor data in the spacelike region. (The radial wave functions are described later). Its behavior in that region was tested by taking it to the lattice QCD regime [34, 35], and also to the nuclear medium [38], both implemented with success.

However, some discussion is necessary for the timelike situation  $q^2 > 0$ . As seen from Eq. (4.5), singularities will appear when  $q^2 = m_{v\pm}^2$ . Physically they correspond to the  $\rho$  and  $\omega$  poles. Another singularity appears from the pole at  $q^2 = M_h^2$ , but only for very large  $q^2$  ( $\simeq 3.5$  GeV<sup>2</sup>). The  $M_h$ -pole was introduced for phenomenological reasons to parametrize the short range physics in the spacelike region [21]. For calculations with large  $W$  (large  $q^2$ ) the  $M_h$ -pole has to be regularized as discussed in the Appendix.

The spacelike parametrization of the quark current in terms of the  $\omega$  and  $\rho$  poles assumes that those particles are stable particles with zero decay width  $\Gamma_v = 0$ . In the extension of the quark form factors to the timelike regime we give them a width and use instead the substitution

$$\frac{m_v^2}{m_v^2 - q^2} \rightarrow \frac{m_v^2}{m_v^2 - q^2 - im_v \Gamma_v(q^2)}, \quad (4.6)$$

where the index  $v$  is used for either  $\rho$  or  $\omega$  as before. In r.h.s.  $\Gamma_v$  denotes the vector meson decay width function in terms of  $q^2$ .

In the application to the  $\Delta(1232)$  Dalitz decay [7] only the  $\rho$  pole was taken because in the  $\gamma^* N \rightarrow \Delta$  transition only the isovector components contribute (given by the functions  $f_{i-}$ ).

The function  $\Gamma_{\rho}(q^2)$  represents the  $\rho \rightarrow 2\pi$  decay width for a virtual  $\rho$  with momentum  $q^2$  [44, 45]

$$\Gamma_{\rho}(q^2) = \Gamma_{\rho}^0 \frac{m_{\rho}^2}{q^2} \left( \frac{q^2 - 4m_{\pi}^2}{m_{\rho}^2 - 4m_{\pi}^2} \right)^{\frac{3}{2}} \theta(q^2 - 4m_{\pi}^2), \quad (4.7)$$

where  $\Gamma_{\rho}^0 = 0.149$  GeV.

For the application in this paper, however, we also have to include the  $\omega$  pole. To this end, the function  $\Gamma_{\omega}(q^2)$  will include the decays  $\omega \rightarrow 2\pi$  (function  $\Gamma_{2\pi}$ ) and  $\omega \rightarrow 3\pi$  (function  $\Gamma_{3\pi}$ ). The case  $\omega \rightarrow 3\pi$  can be interpreted as the process  $\omega \rightarrow \rho\pi \rightarrow 3\pi$ , and therefore we decomposed  $\Gamma_{\omega}(q^2)$  into [44]

$$\Gamma_{\omega}(q^2) = \Gamma_{2\pi}(q^2) + \Gamma_{3\pi}(q^2), \quad (4.8)$$

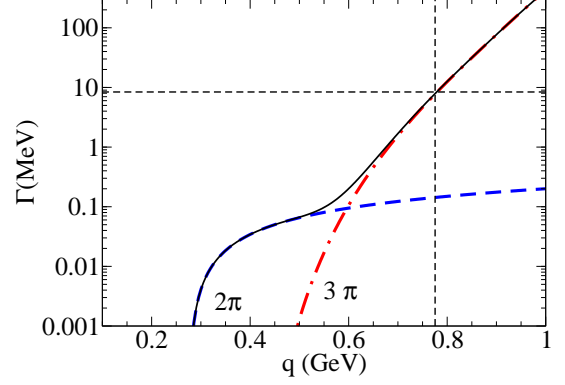


FIG. 1:  $\Gamma_{\omega}$  as a function of  $q$ . The  $2\pi$ ,  $3\pi$  channels are indicated by the long-dashed and dotted-dashed lines respectively. The solid line represents the sum of the two channels. The short-dashed vertical and horizontal lines indicate the  $\omega$  mass point and the  $\omega$ -physical width (8.4 MeV).

The function  $\Gamma_{2\pi}$  can be represented as [44, 46]

$$\Gamma_{2\pi}(q^2) = \Gamma_{2\pi}^0 \frac{m_{\omega}^2}{q^2} \left( \frac{q^2 - 4m_{\pi}^2}{m_{\omega}^2 - 4m_{\pi}^2} \right)^{\frac{3}{2}} \theta(q^2 - 4m_{\pi}^2), \quad (4.9)$$

where  $\Gamma_{2\pi}^0 = 1.428 \times 10^{-4}$  GeV. Note that  $\Gamma_{2\pi}$  is similar to the function  $\Gamma_{\rho}$  except for the constant  $\Gamma_{2\pi}^0$  (about  $10^3$  smaller) and the mass. For the function  $\Gamma_{3\pi}$  we use the result from Ref. [44]

$$\Gamma_{3\pi}(q^2) = \int_{9m_{\pi}^2}^{(q-m_{\pi})^2} ds \mathcal{A}_{\rho}(s) \bar{\Gamma}_{\omega \rightarrow \rho\pi}(q^2, s), \quad (4.10)$$

where  $q = \sqrt{q^2}$ ,  $s$  the mass of the virtual  $\rho$  meson,  $\bar{\Gamma}_{\omega \rightarrow \rho\pi}$  is the decay width of  $\omega$  to a  $\pi$  and a virtual  $\rho$  and  $\mathcal{A}_{\rho}$  is the  $\rho$ -spectral function. The functions  $\bar{\Gamma}_{\omega \rightarrow \rho\pi}$  and  $\mathcal{A}_{\rho}$  are [44]

$$\bar{\Gamma}_{\omega \rightarrow \rho\pi}(q^2, s) = \frac{3}{4\pi} \left( \frac{g'}{m_{\pi}} \right)^2 \left[ \frac{(q^2 - s - m_{\pi}^2)^2 - 4sm_{\pi}^2}{4q^2} \right]^{\frac{5}{2}} \times \theta(q^2 - 9m_{\pi}^2), \quad (4.11)$$

with  $g' = 10.63$  MeV and

$$\mathcal{A}_{\rho}(s) = \frac{\sqrt{s}}{\pi} \frac{\Gamma_{\rho}(s)}{(s - m_{\rho}^2)^2 + s\Gamma_{\rho}^2(s)}. \quad (4.12)$$

With this parametrization we obtain  $\Gamma_{\omega}(m_{\omega}^2) \simeq \Gamma_{3\pi}(m_{\omega}^2) = 7.6$  MeV, which is consistent with the data. Note that the total width of the  $\omega$  comprises the decays into  $\gamma\pi, 2\pi$  and  $3\pi$ , and is 8.4 MeV. The remaining contribution to the  $\omega$  decay width comes from the decay  $\omega \rightarrow \gamma\pi^0$ . The  $3\pi$  decay corresponds to a branching ratio of about 90%.

The result of the calculation of  $\Gamma_{\omega}$  as a function of  $q$  is shown in Fig. 1. Note in this figure the dominance of the  $3\pi$  channel for  $q > 0.55$  GeV.

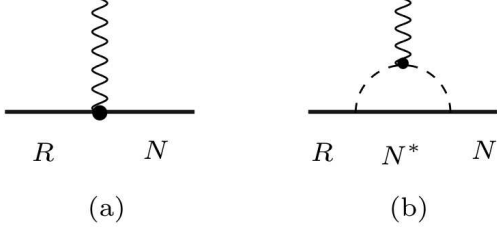


FIG. 2: Electromagnetic interaction with the quark core (a) and with the meson cloud (b). The intermediate  $N^*$  is a octet baryon member (spin 1/2) or a decuplet baryon member (spin 3/2).

## V. FORM FACTORS

Although the  $\gamma^*N \rightarrow N^*(1520)$  transition is characterized by the three independent form factor functions  $G_M, G_E$  and  $G_C$ , in the study of the reaction in the spacelike regime [20] we concluded that it is convenient to define an auxiliary form factor

$$\tilde{G}_4 = G_E + G_M, \quad (5.1)$$

because the valence quark contributions for  $\tilde{G}_4$  are zero and a direct extraction of the *pure* meson cloud contribution from data therefore arises naturally (in the context of the covariant spectator quark model). The valence quark contributions for the transition form factors are discussed next.

Separating the valence quark contribution, represented in Fig. 2(a), from the meson cloud contribution, represented in Fig. 2(b), one can decompose each of the three form factors as in Ref. [20]

$$G_M(q^2, W) = G_M^B(q^2, W) + G_M^\pi(q^2), \quad (5.2)$$

$$G_E(q^2, W) = -G_M^B(q^2, W) - G_M^\pi(q^2) + \tilde{G}_4^\pi(q^2), \quad (5.3)$$

$$G_C(q^2, W) = G_C^B(q^2, W) + G_C^\pi(q^2), \quad (5.4)$$

where  $G_X^B(q^2, W)$ ,  $X = M, E, C$  give the valence quark core contributions and  $G_M^\pi, \tilde{G}_4^\pi$  and  $G_C^\pi$  stand for the matching meson cloud contributions. The label  $\pi$  is used instead of  $MC$  (meson cloud) because we describe those contributions in terms of the pion electromagnetic form factor (following what was done for the  $\gamma^*N \rightarrow \Delta$  transition [7, 20]). The formulas for the valence quark core and meson cloud contributions will be given in the next sections.

Once the transition form factors are known, the helicity amplitudes can be calculated using

$$A_{1/2} = \frac{1}{F} G_M + \frac{1}{4F} \tilde{G}_4, \quad (5.5)$$

$$A_{3/2} = \frac{\sqrt{3}}{4F} \tilde{G}_4, \quad (5.6)$$

$$S_{1/2} = \frac{1}{\sqrt{2}F} \frac{|\mathbf{q}|}{2W} G_C, \quad (5.7)$$

where  $F = \frac{1}{e} \frac{W}{|\mathbf{q}|} \sqrt{\frac{MK}{W} \frac{y_-}{(W-M)^2}}$  with  $K = \frac{W^2 - M^2}{2W}$ .

## A. Valence quark form factors

The contributions of the valence quark core to the form factors can be calculated and seen to have the general final form [9, 47]

$$G_M^B = -\mathcal{R} [(W - M)^2 - q^2] \frac{G_1}{W}, \quad (5.8)$$

$$G_E^B = -\mathcal{R} \left\{ 4G_4 - [(W - M)^2 - q^2] \frac{G_1}{W} \right\}, \quad (5.9)$$

$$G_C^B = -\mathcal{R} [4WG_1 + (3W^2 + M^2 - q^2)G_2 + 2(W^2 - M^2 + q^2)G_3], \quad (5.10)$$

where  $G_i$  ( $i = 1, 2, 3$ ) are three independent form factors and  $\mathcal{R} = \frac{1}{\sqrt{6}} \frac{M}{W - M}$ . The function  $G_4$  was introduced for convenience. Because of current conservation  $G_4$  is given in terms of three independent  $G_i$  ( $i = 1, 2, 3$ ) as [20]

$$G_4 = (W - M)G_1 + \frac{1}{2}(W^2 - M^2)G_2 + q^2G_3. \quad (5.11)$$

By combining the results for  $G_E$  and  $G_M$  one concludes that the valence quark core contribution for  $\tilde{G}_4$  is  $\tilde{G}_4^B = G_E^B + G_M^B = -4\mathcal{R}G_4$ .

The explicit calculation of the form factors requires the determination of the coefficients of the anti-symmetric ( $A$ ) and symmetric ( $S$ ) components of the wave functions, in terms of the quark form factors

$$j_i^A = \frac{1}{6}f_{i+} + \frac{1}{2}f_{i-}\tau_3, \quad (5.12)$$

$$j_i^S = \frac{1}{6}f_{i+} - \frac{1}{6}f_{i-}\tau_3. \quad (5.13)$$

See Refs. [20, 36] for more details.

Then, the functions  $G_i$  can be computed from the nucleon and resonance wave functions. The results are [20]

$$G_1 = -\frac{3}{2\sqrt{2}|\mathbf{q}|} \times \left[ \left( j_1^A + \frac{1}{3}j_1^S \right) + \frac{W + M}{2M} \left( j_2^A + \frac{1}{3}j_2^S \right) \right] \mathcal{I}, \quad (5.14)$$

$$G_2 = \frac{3}{2\sqrt{2}M|\mathbf{q}|} \times \left[ j_2^A + \frac{1}{3} \frac{1 - 3\tau}{1 + \tau} j_2^S + \frac{4}{3} \frac{2M}{W + M} \frac{1}{1 + \tau} j_1^S \right] \mathcal{I}, \quad (5.15)$$

$$G_3 = \frac{3}{2\sqrt{2}|\mathbf{q}|} \frac{W - M}{q^2} \times \left[ j_1^A + \frac{1}{3} \frac{\tau - 3}{1 + \tau} j_1^S + \frac{4}{3} \frac{W + M}{2M} \frac{\tau}{1 + \tau} j_2^S \right] \mathcal{I}, \quad (5.16)$$

where  $\tau = -\frac{q^2}{(W+M)^2}$ , and

$$\mathcal{I} = - \int_k \frac{(\varepsilon_{0P_+} \cdot \tilde{k})}{\sqrt{-\tilde{k}^2}} \psi_R(P_+, k) \psi_N(P_-, k). \quad (5.17)$$

The functions  $\psi_N$  and  $\psi_R$  in the formulas above are the nucleon and resonance radial wave functions, respectively;  $\varepsilon_{0P_+}$  is the spin-1 polarization vector and  $\tilde{k} = k - \frac{P_+ \cdot k}{W^2} P_+$  [20]. The previous integral is calculated in the resonance rest frame using the conditions given by Eqs. (4.3).

From Eq. (5.11) one concludes, as mentioned before, that  $G_4 \equiv 0$ , implying that  $G_E^B = -G_M^B$ , and motivating the use of  $\tilde{G}_4$  to extract direct information on the meson cloud since it, alone, contributes to  $\tilde{G}_4$ .

The consequence of the gauge invariant correction to Eq. (4.1) is that in the Dirac part of the current,  $G_3$  is determined from  $G_1$  and  $G_2$ , and  $G_3$  becomes non-zero at  $q^2 = 0$  [20]. Importantly, the Dirac contribution for  $G_3$  is responsible for the non-vanishing value of  $G_C$  at  $q^2 = 0$ . This is similar to the  $\Delta(1232)$  case addressed in Ref. [23].

The radial wave functions  $\psi_N$  and  $\psi_R$  are parametrized phenomenologically as in Ref. [20] for the  $N^*(1520)$  resonance, and as in Ref. [21] for the nucleon. Those functions depend on  $P \cdot k$ , where  $P$  is the momentum of the baryon. More specifically, those functions can be expressed as functions of the dimensionless variable  $\chi$  which in the nonrelativistic limit becomes proportional to  $\mathbf{k}^2$  [26] and is defined as

$$\chi_B = \frac{(M_B - m_D)^2 - (P - k)^2}{M_B m_D}, \quad (5.18)$$

where  $M_B$  is the mass of the baryon.

The nucleon radial wave function is represented as [21]

$$\psi_N(P, k) = \frac{N_0}{m_D(\beta_1 + \chi_N)(\beta_2 + \chi_N)}, \quad (5.19)$$

where  $\beta_1$  and  $\beta_2$  are two momentum range parameters and  $N_0$  is the normalization constant. We choose  $\beta_2 > \beta_1$ , therefore  $\beta_2$  regulates the long range behavior in the configuration space. In the numerical calculations we used  $\beta_1 = 0.049$  and  $\beta_2 = 0.717$  [21].

For the  $N^*(1520)$  state we used [20]

$$\psi_R(P, k) = \frac{N_1}{m_D(\beta_2 + \chi_R)} \left[ \frac{1}{(\beta_1 + \chi_R)} - \frac{\lambda_R}{(\beta_3 + \chi_R)} \right], \quad (5.20)$$

where  $N_1$  is the normalization constant,  $\beta_3$  is a new (short range) parameter, and  $\lambda_R$  is a parameter determined by an orthogonality condition between the nucleon and the  $N^*(1520)$  wave functions. As in Ref. [20] we use here  $\beta_3 = 0.257$ . The orthogonality condition for wave functions of the nucleon and its excitation is given by  $\mathcal{I}(0) = 0$ , where  $\mathcal{I}(Q^2)$  is defined by Eq. (5.17) [20].

The parameters of the nucleon radial wave function were determined by the direct fit to the nucleon form factor data, in a model with no meson cloud [21]. The parameters of the  $N^*(1520)$  radial wave function were determined by the fit to the  $\gamma^* N \rightarrow N^*(1520)$  data for  $Q^2 = -q^2 > 1.5 \text{ GeV}^2$ , a region where the meson cloud effects are expected to be very small [20].

The radial wave functions  $\psi_N$  and  $\psi_R$  are normalized, by imposing the conditions ( $B = N, R$ )

$$\int_k |\psi_B(\bar{P}, k)|^2 = 1, \quad (5.21)$$

where  $\bar{P} = (M_B, 0, 0, 0)$  is the baryon momentum in the rest frame ( $M_N$  represents the nucleon mass). Equation (5.21) ensures the right charge for each of the baryons  $B$ , obtained from the operator  $\frac{1}{2}(1 + \tau_3)$  [20, 21].

## B. Meson cloud form factors

The meson cloud form factors can be represented as in Ref. [20]

$$\tilde{G}_4^\pi(q^2) = \lambda_\pi^{(4)} \left( \frac{\Lambda_4^2}{\Lambda_4^2 - q^2} \right)^3 F_\pi(q^2) \tau_3, \quad (5.22)$$

$$G_M^\pi(q^2) = (1 - a_M q^2) \times \lambda_\pi^M \left( \frac{\Lambda_M^2}{\Lambda_M^2 - q^2} \right)^3 F_\pi(q^2) \tau_3, \quad (5.23)$$

$$G_C^\pi(q^2) = \lambda_\pi^C \left( \frac{\Lambda_C^2}{\Lambda_C^2 - q^2} \right)^3 F_\pi(q^2) \tau_3, \quad (5.24)$$

where  $F_\pi(q^2)$  is a parametrization of the pion electromagnetic form factors determined in Ref. [7]. Specifically, we use the form

$$F_\pi(q^2) = \frac{\alpha}{\alpha - q^2 - \frac{1}{\pi} \beta q^2 \log \frac{q^2}{m_\pi^2} + i\beta q^2}, \quad (5.25)$$

where  $\alpha = 0.696 \text{ GeV}^2$ ,  $\beta = 0.178$ , and  $m_\pi$  is the pion mass.

In our first work in Ref. [20] the meson cloud was different than the one that we are using here. The reason is that the meson model associated with the diagram Fig. 2(b) was, meanwhile, reparametrized in Ref. [7] to fix the incorrect position of the rho mass pole given by our first model, as well as by other popular parametrizations [7]. In addition, we notice that in this new parametrization the  $\gamma^* N \rightarrow \Delta$  transition pion cloud is directly connected to the pion electromagnetic form factor  $F_\pi(q^2)$ , which is well-established experimentally in the timelike region [7].

The parameters used in the formulas (5.22)-(5.24) were determined by their fit to the  $\gamma^* N \rightarrow N^*(1520)$  spacelike form factors, giving  $a_M = 5.531 \text{ GeV}^{-2}$ ,  $\lambda_\pi^{(4)} = -1.019$ ,  $\lambda_\pi^M = -0.323$ ,  $\lambda_\pi^C = -1.678$ ,  $\Lambda_4^2 = 10.2 \text{ GeV}^2$ ,  $\Lambda_M^2 = 1.241 \text{ GeV}^2$  and  $\Lambda_C^2 = 1.263 \text{ GeV}^2$ . The results are presented in Fig. 3 as a function of  $Q^2 = -q^2$  and compared

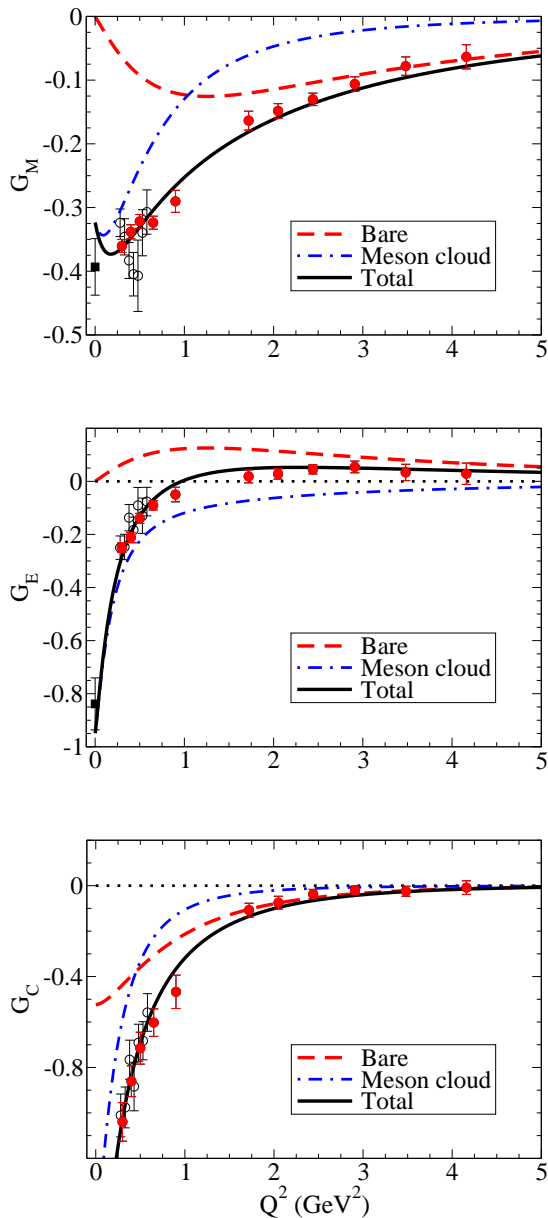


FIG. 3: Valence quark core plus meson cloud contributions to the spacelike form factors as a function of  $Q^2 = -q^2$ . Data from Ref. [48] (full circles), Ref. [49] (empty circles) and PDG [50] (square).

with the spacelike data [48–50]. Check Ref. [20] for a more detailed discussion of the data. In the figure we also show the the valence quark contributions (dashed line) and the meson cloud contributions (dashed-dotted line) based on the parametrizations described above.

In the Appendix, we discuss the technical aspects of the regularization of the singularities appearing in the multipoles of Eqs. (5.22)-(5.24).

## VI. RESULTS

We present in this section our predictions for the  $\gamma^*N \rightarrow N^*(1520)$  transition form factors in the timelike region. Using these results, we also calculate the  $\gamma N$  and  $e^+e^-N$  decay widths.

### A. Form factors

The predictions for the absolute values of the form factors  $G_M$ ,  $G_E$  and  $G_C$  in the timelike region are presented in Fig. 4 for the cases  $W = 1.52, 1.8$  and  $2.1$  GeV. The valence quark core contributions are given by the thin lines. They stand very near the horizontal axis, and vanish in the upper limit  $q^2 = (W - M)^2$  by kinematic constraints. The same result was observed in the quadrupole form factors of the  $\gamma^*N \rightarrow \Delta(1232)$  transition for the physical case, when  $W = M_\Delta \simeq 1.232$  GeV [51].

Figure 4 shows that the meson cloud contribution largely dominates. Only near the  $\omega$ -pole ( $q^2 \simeq 0.6$  GeV<sup>2</sup>) is there a significant contribution from the quark core for the absolute value of the form factors  $G_M$  and  $G_E$ . This effect is very concentrated near  $q^2 \simeq m_\omega^2$  as a consequence of the small  $\omega$  width,  $\Gamma_\omega(m_\omega^2)$ .

In  $G_C$  the effect of the  $\omega$  pole is not observed. This is due to the cancellation of the isoscalar contributions to the form factor  $G_C$ . This cancellation is obtained analytically and can be confirmed by substituting the form factors  $G_1, G_2, G_3$  given by Eqs. (5.14)-(5.16) into the formula of Eq. (5.10) for  $G_C$ . One concludes that only the quark isovector form factors,  $f_{1-}$  and  $f_{2-}$ , contribute to  $G_C$ .

From Fig. 4 one concludes that a fairly good description of the  $\gamma^*N \rightarrow N^*(1520)$  transition can be obtained without the valence quark core contributions, which are very small. The almost perfect coincidence, both for  $G_M$  and  $G_E$ , of the lines corresponding to different values of  $W$  is also a consequence of the dominance of the meson cloud component, since only the valence part depends on  $W$ . Only for  $G_C$  can one distinguish a slight  $W$  dependence, and this is evident because the valence quark contributions are nonzero when  $q^2 = 0$ . The main role of the mass dependence  $W$  in the behavior of the form factors is then to constrain them for  $q^2 \leq (W - M)^2$ .

Qualitatively, one can say that the form factors are enhanced around the origin up to a certain maximum value of  $q^2$ . For  $W = 2.1$  GeV, the magnitude of the form factors starts to decrease after  $q^2 \approx 1$  GeV<sup>2</sup>. This effect is a consequence of the meson cloud parametrization by Eqs. (5.22)-(5.24), which includes a cutoff for  $q^2$  around 1.2 GeV<sup>2</sup>. For larger values of  $W$ , the falloff of the form factors can also be observed.

The impact of the transition form factors in the timelike reactions is determined by the absolute value of  $|G_T(q^2, W)|$  given by Eq. (3.3). The results for  $|G_T(q^2, W)|$  for  $W = 1.52, 1.8$  and  $2.1$  GeV are presented in Fig. 5. There is an increase of  $|G_T(q^2, W)|$  relative to

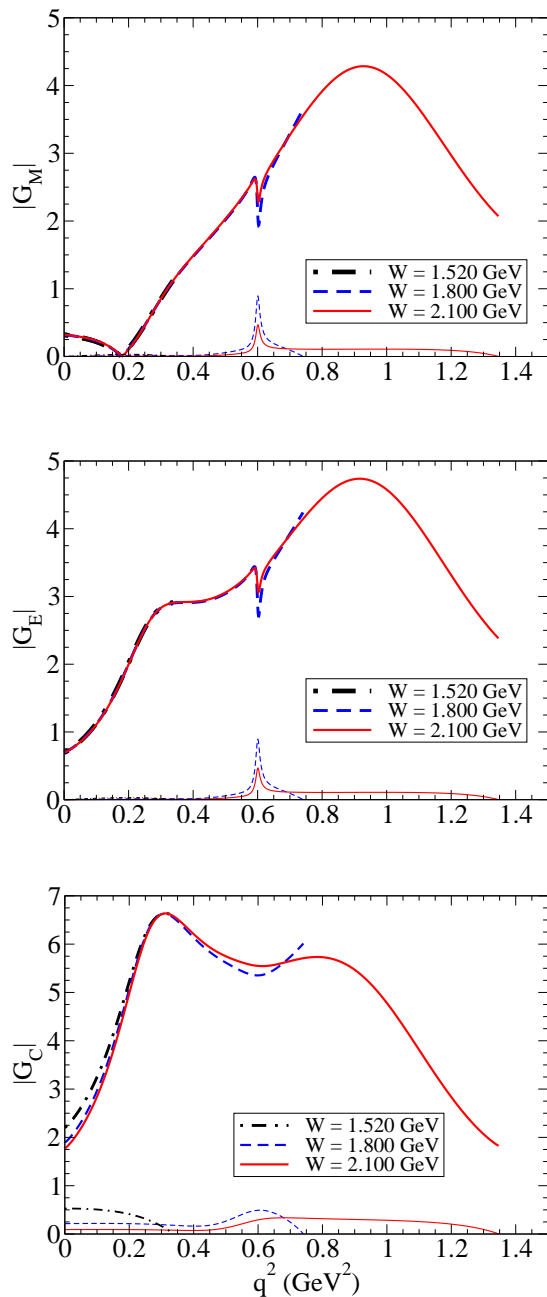


FIG. 4: Absolute values of the form factors for  $W = 1.520, 1.800$  and  $2.100$  GeV. In the calculations we use the new parametrization and the width  $\Gamma_\omega(q^2)$  given by Eq. (4.8). The thin lines represent the contribution from the core. For the total result (thick lines) the lines for  $W = 1.520$  GeV coincide with the lines for  $W = 1.800$  and  $2.100$  GeV.

its value at the origin up to  $q^2 \simeq 0.9$  GeV<sup>2</sup>, for  $W > 1.8$  GeV. Above  $q^2 = 0.9$  GeV<sup>2</sup> one gets a first glance at the expected falloff for the form factors mentioned previously.

The function  $|G_T(q^2, W)|$ , particularly how it evolves away from  $q^2 = 0$ , has important consequences for the  $N^*(1520) \rightarrow \gamma^* N$  transition. In general, the  $N^* \rightarrow \gamma^* N$  reactions are often studied under the assumption that

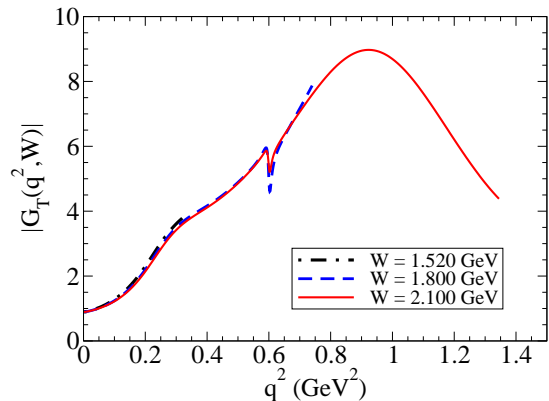


FIG. 5: Effective contribution of the form factors  $|G_T(q^2, W)|$  for  $W = 1.520, 1.800$  and  $2.100$  GeV.

the transition form factors in the timelike region can be approximated by the experimental value of the form factors at the photon point ( $q^2 = 0$ ), which implies that  $W$  is fixed by the physical mass of the resonance — and therefore there is no  $W$  dependence. In the literature this approximation (no  $q^2$  dependence of the electromagnetic coupling and  $W = M_R$ ) is known as the *QED approximation*, and it represents the form factor of a pointlike particle. We also refer to this approximation as the constant form factor model. By construction, the constant form factor model is not constrained by the form factor  $G_C$ , because, at  $q^2 = 0$ ,  $G_C$  does not contribute to  $|G_T|^2$ , according to Eq. (3.3). For finite  $q^2$ , however,  $G_C$  contributes to  $|G_T|^2$  with the term  $\frac{q^2}{2W^2}|G_C|^2$ .

In Fig. 5 one can see that the value of  $|G_T|$  at  $q^2 = 0$  is close to 1, consistently with the experimental value. Therefore, in the constant form factor model,  $|G_T| \equiv 1.048$  underestimates the results from Fig. 5. Taking, for instance  $q^2 = 0.9$  GeV, where  $|G_T| \simeq 9$ , one concludes that in the constant form factor model  $|G_T|$  is about an order of magnitude too low. Since the impact of  $|G_T|$  in the decay widths is proportional to  $|G_T|^2$ , in the range  $q^2 = 0-1$  GeV<sup>2</sup> the constant form factor model may underestimate the decay widths in 1 or 2 orders of magnitude. For larger values of  $q^2$ , however, the discussion is different, since in our model,  $|G_T|^2$  goes down with  $q^2$  due to the multipole parametrizations of the meson cloud component.

The meson cloud dominance can be physically understood in terms of the decay mechanisms of the resonances  $N^*(1520)$  and  $\Delta(1232)$ . The  $\Delta(1232)$  decays almost exclusively into  $\pi N$ , but the  $N^*(1520)$  can decay into  $\pi N$  (40%) and into  $\pi\pi N$  (60%) [50]. From the  $\pi\pi N$  decays, one can expect then a stronger contribution from the meson cloud effects for the transition form factors for the  $N^*(1520)$  than for the  $\Delta(1232)$ . The strength of these  $\pi\pi N$  decays is encoded in the form factor data that we use in our fit to the physical spacelike form factor data. In the  $\gamma^* N \rightarrow \Delta(1232)$  transition, the leading form fac-



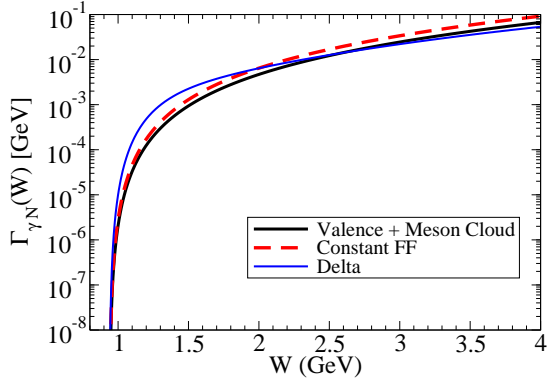


FIG. 6: Decay width  $\Gamma_{\gamma N}$  as function of  $W$ . The current model (Valence + Meson Cloud) is compared with the constant form factor model and with the results obtained for the  $\Delta(1232)$  (see Ref. [7]).

tor is the magnetic form factor, and in ours and other calculations, it is dominated by the valence quark contributions at low  $q^2$  [6, 7, 22, 23]. There is, therefore, a smaller impact from the pion cloud. By contrast, for the  $\gamma^* N \rightarrow N^*(1520)$  transition, the electric and the magnetic form factors are both relevant at low  $q^2$ . It is the different structure of form factors for the  $\gamma^* N \rightarrow N^*(1520)$  and  $\gamma^* N \rightarrow \Delta(1232)$  transition that implies a dominance of the meson cloud effects, in the first case.

### B. Calculation of the decay width $\Gamma_{\gamma N}(W)$

Using the formalism in Sec. III, we calculate the  $N^*(1520) \rightarrow \gamma N$  decay width as a function of  $W$ . The  $\gamma N$  decay width ( $\Gamma_{\gamma N}$ ) is determined by the function  $\Gamma_{\gamma^* N}(q, W)$ , given by Eq. (3.1) in the limit  $q^2 = 0$ . This width is then proportional to the function  $|G_T(0, W)|^2$ .

Our results for  $\Gamma_{\gamma N}(W)$  are presented in Fig. 6 (thick solid line). Since, as observed for the form factors, the dependence of  $|G_T|$  on  $W$  is weak, the shape of  $\Gamma_{\gamma N}(W)$  is determined mainly by the kinematic factor multiplying  $|G_T|^2$  in Eq. (3.1). The results are also compared with the constant form factor model (dashed line). In the figure the results from the constant form factor for  $\Gamma_{\gamma N}(W)$  are close to the  $q^2$  dependent results, but we note that a logarithmic representation is used. The deviation for large  $W$  is about 30%. The similarity between the two results comes from the small dependence of our model on  $W$  in the limit  $q^2 \rightarrow 0$ . We expect that for observables depending on  $q^2$  the results will differ much more. This is indeed the case, as confirmed in the next section.

To close this section, we compare  $\Gamma_{\gamma N}(W)$  with the  $\Delta(1232) \rightarrow \gamma N$  decay width calculated in the Ref. [7] also within the covariant spectator quark model framework (thin solid line). It is interesting that the  $\Delta$  decay width is larger for small values of  $W$ , but the  $N^*(1520)$  decay width is larger when  $W > 2.5$  GeV.

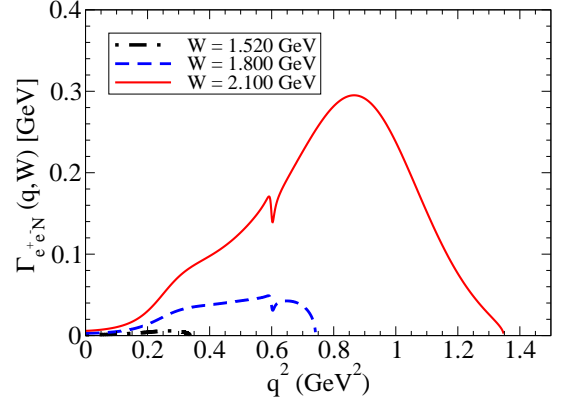


FIG. 7: Dalitz decay width  $\Gamma_{e^+e^-N}(q^2, W)$  for  $W = 1.520, 1.800$  and  $2.100$  GeV.

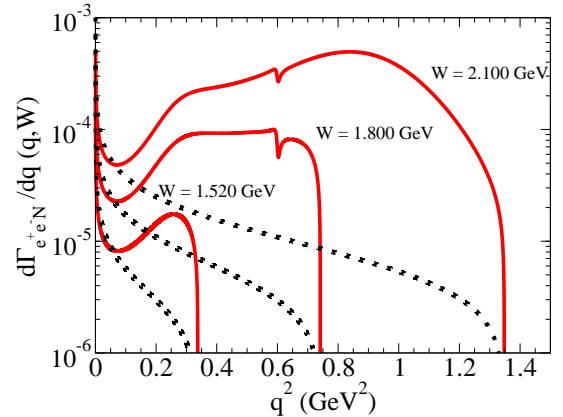


FIG. 8: Results of  $\frac{d\Gamma}{dq}$  for  $W = 1.520, 1.800$  and  $2.100$  GeV (solid lines), compared to the estimate from the constant form factor model (dotted lines).

### C. $N^*(1520)$ Dalitz decay

We show now the results for the  $N^*(1520)$  Dalitz decay,  $N^*(1520) \rightarrow e^+e^-N$ . The Dalitz decay width is determined by the function  $\Gamma_{\gamma^* N}(q, W)$ , given by Eq. (3.1) for the case where  $q^2$  is the photon momentum transfer for the dilepton decay  $\gamma^* \rightarrow e^+e^-$ .

In Fig. 7, we present the results of  $\Gamma_{\gamma^* N}(q, W)$  for  $W = 1.52, 1.8$  and  $2.1$  GeV. The dependence of  $\Gamma_{\gamma^* N}$  on both variables,  $q^2$  and  $W$ , is clear from the figure

Finally we show the dilepton decay rate  $\frac{d\Gamma}{dq}(q, W)$ , where as before, we use the notation  $\Gamma(q, W) \equiv \Gamma_{e^+e^-N}(q, W)$ . The results for  $\frac{d\Gamma}{dq}$  for the three values of  $W$  discussed previously are presented in Fig. 8. The results are compared with the constant form factor model. The covariant spectator quark model differs significantly from the constant form factor model for  $q^2 > 0.1$  GeV<sup>2</sup>. This effect is caused by the meson cloud contributions included in our model.

The function  $\Gamma_{e^+e^-N}(W)$  can now be evaluated inte-

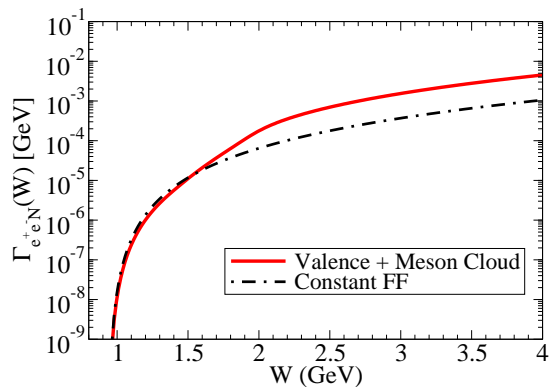


FIG. 9:  $N^*(1520)$  Dalitz decay width as a function of  $W$ . The result of our model (solid line) is compared with the result of the constant form factor model (dotted-dashed line).

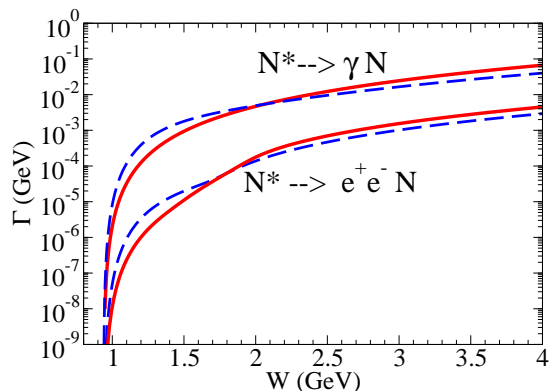


FIG. 10:  $N^*(1520)$  decay widths as function of  $W$ . Photon and Dalitz decays (solid lines). The results are also compared to the calculation for the  $\Delta(1232)$  case (dashed lines).

grating in  $q$  according to Eq. (3.5). The results are presented in Fig. 9 that shows also the comparison with the results obtained with the constant form factor model. From the figure we can conclude that the effect of the  $q^2$  dependence is diluted when we integrate in  $q$  for  $W < 1.6$  GeV. One concludes then that the  $q^2$  dependence on  $|G_T|^2$  is important when we look for the function  $\Gamma_{e^+e^-N}(q, W)$ , or for  $\Gamma_{e^+e^-N}(W)$  at a large  $W$ .

In Fig. 10 we present the results of  $\Gamma_{e^+e^-N}(W)$  in comparison to the electromagnetic decay width  $\Gamma_{\gamma N}(W)$ . In the same figure, we compare also our results for  $\Gamma_{e^+e^-N}(W)$ ,  $\Gamma_{\gamma N}(W)$  from the  $N^*(1520)$  resonance with the corresponding ones from the  $\Delta(1232)$  decays [7]. In both cases, one includes the combination of the valence quark and meson cloud contributions.

The results from Fig. 10 imply that the two resonances are almost equally relevant for a large  $W$ , suggesting that the  $N^*(1520)$  may play an important role in dilepton decay reactions.

## VII. OUTLOOK AND CONCLUSIONS

We apply to the  $N^*(1520) \rightarrow \gamma N$  transition a model which adds a covariant valence quark core contribution with a meson cloud term. The meson cloud term is related to the pion electromagnetic form factor, which is well-established in the timelike region, and the transition form factors are first fixed in the spacelike region. The form factor behavior in the timelike region is then predicted, as well as the  $N^*(1520) \rightarrow \gamma N$  decay width and the  $N^*(1520)$  Dalitz decay,  $N^*(1520) \rightarrow e^+e^-N$ . The timelike  $N^*(1520)$  transition form factors are dominated by the meson cloud contributions.

In the range  $q^2 = 0-1$  GeV<sup>2</sup> the constant form factor model or *QED approximation* that is usually taken in the literature underestimates the electromagnetic coupling of the  $N^*(1520)$  up to 2 orders of magnitude. This has a large effect on  $q^2$  dependent observables as the  $N^*(1520)$  Dalitz decay. The  $q^2$  dependence effect may be diluted in  $\Gamma_{e^+e^-N}(W)$  which is obtained by integrating over  $q^2$ , but it can be clearly observed if we look at the differential Dalitz decay width  $\frac{d\Gamma}{dq}(q, W)$ .

In line with the HADES results [3, 13, 14], the  $N^*(1520)$  and  $\Delta(1232)$  decays compete, and at large energies the first is certainly important.

## Acknowledgments

G.R. was supported by the Brazilian Ministry of Science, Technology and Innovation (MCTI-Brazil). M.T.P. received financial support from Fundação para a Ciência e a Tecnologia (FCT) under Grants Nos. PTDC/FIS/113940/2009, CFTP-FCT (PEst-OE/FIS/U/0777/2013) and POCTI/ISFL/2/275. This work was also partially supported by the European Union under the HadronPhysics3 Grant No. 283286.

## Appendix A: Regularization of high momentum poles

As discussed in the main text, for a given  $W$  the squared momentum  $q^2$  is limited by the condition  $q^2 \leq (W - M)^2$ . Then, if one has a singularity for  $q^2 = \Lambda^2$ , that singularity will appear for values of  $W$  such that  $\Lambda^2 \leq (W - M)^2$ , or  $W \geq M + \Lambda$ .

To avoid a singularity at  $q^2 = \Lambda^2$ , where  $\Lambda^2$  is one of the cutoffs introduced in our meson cloud parametrizations and in the quark current (pole at  $q^2 = M_h$ ) we will use a simple procedure. We start with

$$\frac{\Lambda^2}{\Lambda^2 - q^2} \rightarrow \frac{\Lambda^2}{\Lambda^2 - q^2 - i\Lambda\Gamma_X(q^2)}, \quad (\text{A1})$$

where

$$\Gamma_X(q^2) = 4\Gamma_X^0 \left( \frac{q^2}{q^2 + \Lambda^2} \right)^2 \theta(q^2), \quad (\text{A2})$$

In the last equation  $\Gamma_X^0$  is a constant given by  $\Gamma_X^0 = 4\Gamma_\rho^0 \simeq 0.6$  GeV.

The function  $\Gamma_X(q^2)$  defined by Eq. (A2) is  $\Gamma_X(q^2) = 0$  when  $q^2 < 0$ , and continuously extended for  $q^2 > 0$ . Therefore the results in spacelike (where there are no singularities) are kept unchanged. The factor  $4\Gamma_X^0$  was chose in order to obtain  $\Gamma_X = \Gamma_X^0$ , for  $q^2 = \Lambda^2$ , and  $\Gamma_X \simeq 4\Gamma_X^0$  for very large  $q^2$ . Finally the value of  $\Gamma_X^0$  was chosen to avoid very narrow peaks around  $\Lambda^2$ .

Contrarily to the width  $\Gamma_\rho(q^2)$  associated with the  $\rho$ -meson pole in the quark current which has nonzero values only when  $q^2 > 4m_\pi^2$ , one has for  $\Gamma_X(q^2)$  nonzero values also in the interval  $4m_\pi^2 > q^2 > 0$ . However, the function  $\Gamma_X(q^2)$  varies smoothly in that interval and its values are very small when compared to  $\Gamma_X^0$ .

The procedure given by Eqs. (A1)-(A2) was used already in applications of the model from Ref. [6] in the calculation of the  $\gamma^*N \rightarrow \Delta$  form factors in the timelike

regime [7, 17]. With this procedure the emerging singularities for  $W > 2.17$  GeV are avoided and the results are almost identical to the results for  $W < 2.17$  GeV, without regularization. The singularity that appears for  $W \simeq 2.17$  GeV is due to the pion cloud parametrization of  $G_M$  [6].

As in most cases, the high momentum effects and the high  $q^2$  contributions are suppressed, and the details of the regularization procedure are not important, as far as removing the spurious singularities is concerned.

For the tripole factors associated with the functions (5.22)-(5.24) we use

$$\left(\frac{\Lambda^2}{\Lambda^2 - q^2}\right)^3 \rightarrow \left(\frac{\Lambda^4}{(\Lambda^2 - q^2)^2 + \Lambda^2[\Gamma_X(q^2)]^2}\right)^{3/2}, \quad (\text{A3})$$

where  $\Gamma_X(q^2)$  is obtained by Eq. (A2).

- 
- [1] W. J. Briscoe, M. Döring, H. Haberzettl, D. M. Manley, M. Naruki, I. I. Strakovsky and E. S. Swanson, *Eur. Phys. J. A* **51**, 129 (2015) [arXiv:1503.07763 [hep-ph]].
- [2] A. Faessler, C. Fuchs, M. I. Krivoruchenko and B. V. Martemyanov, *J. Phys. G* **29**, 603 (2003) [nucl-th/0010056].
- [3] G. Agakishiev *et al.*, *Eur. Phys. J. A* **50**, 82 (2014) [arXiv:1403.3054 [nucl-ex]]; G. Agakishiev *et al.* [HADES Collaboration], *Eur. Phys. J. A* **48**, 64 (2012) [arXiv:1112.3607 [nucl-ex]].
- [4] G. Agakishiev *et al.* [HADES Collaboration], *Eur. Phys. J. A* **48**, 74 (2012) [arXiv:1203.1333 [nucl-ex]]; G. Agakishiev *et al.* [HADES Collaboration], *Phys. Rev. C* **85**, 054005 (2012) [arXiv:1203.2549 [nucl-ex]]; G. Agakishiev *et al.* [HADES Collaboration], *Eur. Phys. J. A* **51**, 137 (2015).
- [5] G. Agakishiev *et al.* [HADES Collaboration], *Phys. Lett. B* **690**, 118 (2010) [arXiv:0910.5875 [nucl-ex]]; G. Agakishiev *et al.* [HADES Collaboration], *Phys. Lett. B* **715**, 304 (2012) [arXiv:1205.1918 [nucl-ex]].
- [6] G. Ramalho and M. T. Peña, *Phys. Rev. D* **85**, 113014 (2012) [arXiv:1205.2575 [hep-ph]].
- [7] G. Ramalho, M. T. Peña, J. Weil, H. van Hees and U. Mosel, *Phys. Rev. D* **93**, 033004 (2016) [arXiv:1512.03764 [hep-ph]].
- [8] I. G. Aznauryan, A. Bashir, V. Braun, S. J. Brodsky, V. D. Burkert, L. Chang, C. Chen and B. El-Bennich *et al.*, *Int. J. Mod. Phys. E*, Vol. 22, **1330015** (2013) [arXiv:1212.4891 [nucl-th]].
- [9] I. G. Aznauryan and V. D. Burkert, *Prog. Part. Nucl. Phys.* **67**, 1 (2012) [arXiv:1109.1720 [hep-ph]].
- [10] S. Teis, W. Cassing, M. Effenberger, A. Hombach, U. Mosel and G. Wolf, *Z. Phys. A* **356**, 421 (1997) [nucl-th/9609009].
- [11] S. A. Bass *et al.*, *Prog. Part. Nucl. Phys.* **41**, 255 (1998) [*Prog. Part. Nucl. Phys.* **41**, 225 (1998)] [nucl-th/9803035].
- [12] O. Buss *et al.*, *Phys. Rept.* **512**, 1 (2012) [arXiv:1106.1344 [hep-ph]].
- [13] B. Ramstein [HADES Collaboration], *AIP Conf. Proc.* **1735**, 080001 (2016).
- [14] W. Przygoda [HADES Collaboration], *JPS Conf. Proc.* **10**, 010013 (2016).
- [15] E. L. Bratkovskaya, W. Cassing, M. Effenberger and U. Mosel, *Nucl. Phys. A* **653**, 301 (1999) [nucl-th/9903009].
- [16] L. P. Kaptari and B. Kampfer, *Phys. Rev. C* **80**, 064003 (2009) [arXiv:0903.2466 [nucl-th]].
- [17] J. Weil, H. van Hees, and U. Mosel, *Eur. Phys. J. A* **48**, 111 (2012) [Erratum-ibid. *A* **48**, 150 (2012)] [arXiv:1203.3557 [nucl-th]].
- [18] G. Eichmann, H. Sanchis-Alepuz, R. Williams, R. Alkofer and C. S. Fischer, arXiv:1606.09602 [hep-ph].
- [19] F. Gross, *Phys. Rev.* **186**, 1448 (1969); A. Stadler, F. Gross and M. Frank, *Phys. Rev. C* **56**, 2396 (1997). [arXiv:nucl-th/9703043].
- [20] G. Ramalho and M. T. Peña, *Phys. Rev. D* **89**, 094016 (2014) [arXiv:1309.0730 [hep-ph]].
- [21] F. Gross, G. Ramalho and M. T. Peña, *Phys. Rev. C* **77**, 015202 (2008) [nucl-th/0606029].
- [22] G. Ramalho, M. T. Peña and F. Gross, *Eur. Phys. J. A* **36**, 329 (2008) [arXiv:0803.3034 [hep-ph]].
- [23] G. Ramalho, M. T. Peña and F. Gross, *Phys. Rev. D* **78**, 114017 (2008) [arXiv:0810.4126 [hep-ph]].
- [24] F. Gross, G. Ramalho and M. T. Peña, *Phys. Rev. D* **85**, 093006 (2012) [arXiv:1201.6337 [hep-ph]].
- [25] F. Gross, G. Ramalho and M. T. Peña, *Phys. Rev. D* **85**, 093005 (2012) [arXiv:1201.6336 [hep-ph]].
- [26] G. Ramalho, K. Tsushima and F. Gross, *Phys. Rev. D* **80**, 033004 (2009) [arXiv:0907.1060 [hep-ph]].
- [27] G. Ramalho and M. T. Peña, *Phys. Rev. D* **83**, 054011 (2011) [arXiv:1012.2168 [hep-ph]].
- [28] G. Ramalho, M. T. Peña and A. Stadler, *Phys. Rev. D* **86**, 093022 (2012) [arXiv:1207.4392 [nucl-th]]; G. Ramalho, M. T. Peña and F. Gross, *Phys. Rev. D* **81**, 113011 (2010) [arXiv:1002.4170 [hep-ph]]. G. Ramalho and M. T. Peña, *J. Phys. G* **36**, 085004 (2009) [arXiv:0807.2922 [hep-ph]].
- [29] G. Ramalho and K. Tsushima, *Phys. Rev. D* **89**, 073010 (2014) [arXiv:1402.3234 [hep-ph]]; G. Ramalho

- and K. Tsushima, Phys. Rev. D **81**, 074020 (2010) [arXiv:1002.3386 [hep-ph]].
- [30] G. Ramalho and M. T. Peña, Phys. Rev. D **84**, 033007 (2011) [arXiv:1105.2223 [hep-ph]].
- [31] G. Ramalho and K. Tsushima, Phys. Rev. D **82**, 073007 (2010) [arXiv:1008.3822 [hep-ph]].
- [32] G. Ramalho, Phys. Rev. D **90**, 033010 (2014) [arXiv:1407.0649 [hep-ph]].
- [33] G. Ramalho and K. Tsushima, Phys. Rev. D **94**, 014001 (2016) [arXiv:1512.01167 [hep-ph]].
- [34] G. Ramalho and M. T. Peña, J. Phys. G **36**, 115011 (2009) [arXiv:0812.0187 [hep-ph]].
- [35] G. Ramalho and M. T. Peña, Phys. Rev. D **80**, 013008 (2009) [arXiv:0901.4310 [hep-ph]].
- [36] F. Gross, G. Ramalho and K. Tsushima, Phys. Lett. B **690**, 183 (2010) [arXiv:0910.2171 [hep-ph]]; G. Ramalho and K. Tsushima, Phys. Rev. D **84**, 054014 (2011) [arXiv:1107.1791 [hep-ph]].
- [37] G. Ramalho, D. Jido and K. Tsushima, Phys. Rev. D **85**, 093014 (2012) [arXiv:1202.2299 [hep-ph]]; G. Ramalho and K. Tsushima, Phys. Rev. D **86**, 114030 (2012) [arXiv:1210.7465 [hep-ph]]; G. Ramalho and K. Tsushima, Phys. Rev. D **88**, 053002 (2013) [arXiv:1307.6840 [hep-ph]]; G. Ramalho and K. Tsushima, Phys. Rev. D **87**, 093011 (2013) [arXiv:1302.6889 [hep-ph]].
- [38] G. Ramalho, K. Tsushima and A. W. Thomas, J. Phys. G **40**, 015102 (2013) [arXiv:1206.2207 [hep-ph]].
- [39] M. I. Krivoruchenko, B. V. Martemyanov, A. Faessler and C. Fuchs, Annals Phys. **296**, 299 (2002) [arXiv:nucl-th/0110066].
- [40] A. Faessler, C. Fuchs and M. I. Krivoruchenko, Phys. Rev. C **61**, 035206 (2000) [nucl-th/9904024].
- [41] J. J. Kelly, Phys. Rev. C **56**, 2672 (1997).
- [42] Z. Batiz and F. Gross, Phys. Rev. C **58**, 2963 (1998) [arXiv:nucl-th/9803053].
- [43] R. A. Gilman and F. Gross, J. Phys. G **28**, R37 (2002) [nucl-th/0111015].
- [44] P. Mühlich and U. Mosel, Nucl. Phys. A **773**, 156 (2006) [nucl-th/0602054]; P. Mühlich, PhD thesis (2007).
- [45] H. B. O'Connell, B. C. Pearce, A. W. Thomas and A. G. Williams, Phys. Lett. B **354**, 14 (1995) [arXiv:hep-ph/9503332].
- [46] H. B. O'Connell, B. C. Pearce, A. W. Thomas and A. G. Williams, Prog. Part. Nucl. Phys. **39**, 201 (1997) [hep-ph/9501251].
- [47] R. C. E. Devenish, T. S. Eisenschitz and J. G. Korner, Phys. Rev. D **14**, 3063 (1976).
- [48] I. G. Aznauryan *et al.* [CLAS Collaboration], Phys. Rev. C **80**, 055203 (2009) [arXiv:0909.2349 [nucl-ex]].
- [49] V. I. Mokeev *et al.* [CLAS Collaboration], Phys. Rev. C **86**, 035203 (2012) [arXiv:1205.3948 [nucl-ex]].
- [50] J. Beringer *et al.* [Particle Data Group Collaboration], Phys. Rev. D **86**, 010001 (2012).
- [51] G. Ramalho, arXiv:1606.03042 [hep-ph].